



# Journal of Applied Sciences

ISSN 1812-5654

**science**  
alert

**ANSI***net*  
an open access publisher  
<http://ansinet.com>

## Image Processing for Synthesizing Lung Nodules: A Experimental Study

N.S. Raghava and G. Senthil Kumar  
Department of Electronic and Communications Engineering,  
Delhi College of Engineering, New Delhi, India

---

**Abstract:** The aim of this experiment is to study how effectively image processing utilises in CT scan. So a software application is developed using MATLAB software to experiment computer tomography (CT) image, using this application we identify the real nodule and create a 3d mesh Gaussian structure. A Certain parameters of this 3D mesh are taken to create a synthetic lung nodule. This synthetic nodule is inserted into the CT image. The real and synthetic nodules are evaluated from its appearance and shape in the CT image and 3D mesh plot. Based on this, more number of synthetic nodules can be created using various parameters; the characteristics of nodules are stored in to single database, which might be useful to the radiologist for further references of analysing the Lung nodules.

**Key words:** Lung cancer, synthetic nodules, computed tomography image (CT), Matlab

---

### INTRODUCTION

Lung cancer is the most common disease world wide and is the major cause of death from cancer, particularly amongst men. It was a rare disease until the beginning of the 20th century. Since then the occurrence of lung cancer has increased rapidly and it now accounts for an estimated 901,746 new cases each year among men and 337,115 among women (Stewart and Kleihues, 2003). This emphasizes the need for finding ways to improve the diagnosis of lung cancer so it can be caught as early as possible. Early detection is the best way of increasing survival rate for lung cancer patients. On average the five year survival rate of lung cancer patient is 47% patients whose cancer is detected early is 49% (Dajnowiec and Alirezaie, 2004).

Survival from lung cancer is dependent on the stage of the cancer. The stage is determined by the size and location of the tumor, the presence of cancer in the surrounding lymph nodes, and spread to distant sites. When lung cancer is treated in its earliest stage the cure rate approaches 70% or greater. The size of the tumor also impacts on survival, even for tumors discovered at an early stage. The survival is worse for patients whose tumors are greater than 3 cm than for those who have tumors less than 3 cm in size. It remains to be seen whether detection at an even smaller size (less than 3 cm) has an even greater impact on survival (Davies, 1990).

CT screening is the best method to detect lung cancer in its earliest stage (Kanazawa *et al.*, 1998). Since

the majority of lung cancers originate as a small growth, or nodule in the lung, screening CT scans are extremely sensitive in detecting nodules as small as 2 or 3 mm within the lungs. Screening CT scans are capable of detecting lung nodules much smaller than by conventional chest X-ray (Armato *et al.*, 1999). In fact in the recently published articles on CT screening, the majority of lung cancers that were found on CT scanning could not be detected on the chest X-ray that was performed simultaneously. If a nodule is found on a screening CT scan, than a decision is made to either biopsy the nodule if it appears suspicious for cancer, or to repeat a CT scan within 6 to 12 weeks to determine if the nodule has grown. Should the nodule grow, this is highly suspicious for malignancy, and a recommendation to biopsy the nodule is warranted (Zhao *et al.*, 2003). If on the other hand the nodule remains stable in size, and does not change, then continued observation is recommended.

The number of images available to radiologists is growing rapidly (Zrimec and Busayarat, 2004). For example, High Resolution CT (HRCT) imaging protocols of the lungs on single detector scanners typically generate up to 40 images per study, while multi-slice protocols may generate 300-600 high-resolution axial images. Although most lung diseases produce recognizable alteration in the lung anatomy that can be captured by thin-slice CT scans, it is often difficult and time consuming to analyse images accurately and efficiently by hand (Gonzalez and Woods, 1992). Efficient methods for visualization and image interpretation are

required to assist radiologists in focusing their attention on diagnostically interesting events. Such a system should be able to indicate the existence and location of potential abnormalities and to provide measurements and visualization of the size and distribution of abnormalities in order to facilitate diagnosis. Study covers the approach of modeling and visualizing human lung anatomy. The model provides assistance in segmentation and detection of anatomical lung features and patterns of pathology in HRCT lung scans. To facilitate image segmentation and labelling, the model includes both a symbolic representation of the anatomy and a representation in the form of a 3D atlas had been experienced.

A new recognition method of lung nodules from X-ray CT images using 3D Markov random field (MRF) models has been proposed (Takizawa and Yamamoto, 2002). Pathological shadow candidates are detected by a mathematical morphology filter, and volume of interest (VOI) areas, which include the shadow candidates, are extracted. The probabilities of the hypotheses that the VOI areas come from nodules (which are candidates of cancers) and blood vessels are calculated using nodule and blood vessel models evaluating the relations between these object models by 3D MRF models.

Medical images generally provide a “snapshot” of a portion of the patient’s anatomy at a particular moment in time (Bullitt and Aylward, 2001). A second image, taken at a later time, may show obvious differences. Such changes may occur for at least four reasons. First, some image acquisition techniques are dynamic, resulting in a sequence of related images each of which differs from the others. Second, changes between images may result from changes in the image acquisition process, as may occur if the two studies are of different modalities or employ different parameter settings. Third, organs may shift or deform between images as a result of change in the patient’s position, respiratory motion, or an external force such as intraoperative retraction. Finally, changes in image objects over time may occur because the patient’s anatomy has itself changed, as may happen with progression or regression of pathology, or as may occur with operative resection of tissue.

A means of defining tubular objects from 3D image data and of registering such images with other 2- or 3D images that contain at least a subset of the same tubes is discussed. Such registration can provide a means of understanding, interpreting, and analyzing a variety of changes that may occur in images taken over time. An advantage of the approach is that blood vessels exist throughout the human body. The methods outlined here are therefore immediately applicable to a wide variety of

disease processes, to a large range of image modalities, and to almost any anatomical region.

The author proposed (Zwirewich *et al.*, 1991) a recognition method of lung nodules based on experimentally selected feature values (such as contrast, circularities, etc.) of pathological candidate regions detected by our Quoit filter. In this study, we propose a new recognition method of lung nodule using each CT value itself in ROI (region of interest) area as a feature value. In the clustering stage, first, the pathological candidate regions are classified into some clusters using Principal Component (PC) theories. A set of CT values in each ROI is regarded as a feature vector, and then Eigen vectors and Eigen values are calculated for each cluster by applying Principal Component Analysis (PCA). The eigen vectors corresponding to the 10 largest eigen values, are utilized as base vectors for subspaces of the clusters in the feature space. In the discrimination stage, correlations are measured between the testing feature vector and the subspace, which is spanned by the Eigen Images. If the correlation with the abnormal subspace is large, the pathological candidate region is determined to be abnormal. Otherwise, it is determined to be normal. By applying our new method, good results have been acquired.

First, to detect cancer shadows, he proposed an image filter called Quoit filter, which is a type of mathematical morphology filter. This filter can automatically detect abnormal shadows with the sensitivity over 95%, but it detects many false positives, which are mainly related to blood vessel shadows. In order to reduce such false positives, we developed a discrimination method of cancer shadows based on feature values obtained from pathological candidate regions detected. In this method, experiment about 15 types of the feature values such as average CT values, modified circularity, and X ray attenuations are used. However, it could not be guaranteed that they were the optimal combination for recognizing the pathological candidate regions. They also explained a new recognition method using each CT value itself in a ROI area as a feature value. By applying PCA to these CT values, essential information can be extracted from CT images, and the accuracy of our CAD system is increased drastically.

It is mainly focused to characterize the internal intensity and structure of pulmonary nodules in thin-section CT images for classification between benign and malignant nodules (Nakamura *et al.*, 2004). This approach makes use of shape index, curvedness, and CT density to represent locally each voxel constructing the three-dimensional (3D) pulmonary nodule image. From the distribution of shape index, curvedness, and CT density

over the 3D pulmonary nodule image a set of histogram features, and 3D texture features is computed to classify benign and malignant nodules. Linear discriminant analysis is used for classification and a Receiver Operating Characteristic (ROC) analysis is used to evaluate classification accuracy. The potential usefulness of the curvature based features in the computer-aided differential diagnosis is demonstrated by using ROC curves as the performance measure.

Nodule segmentation of the 3D pulmonary nodule image consists of extraction of lung area, Selection of Region Of Interest (ROI) including the nodule region and nodule segmentation based on a geometric approach.

Lung area extraction plays an essential role when part of a nodule in the peripheral lung area touches the chest wall. The ROI including the nodule was selected interactively. A pulmonary nodule was segmented from the selected ROI image by the geometric approach proposed (Caselle *et al.*, 1993). The geometric approach was based on deforming 3D surfaces, represented by level-sets, toward the nodule boundary to be extracted in the 3D chest image. The deformation process of the used 3D deformable surface mode can automatically stop when the deforming surfaces reach the object boundary to be detected. In their application they controlled a stopping condition to exclude vessels and bronchi which contact the pulmonary nodule.

#### MATERIALS AND METHODS FOR SYNTHESIZING LUNG NODULES

CT images of real lung nodule cases formed the basis for the lung nodule insertion technique. The following Fig. 1a shows a CT images with a nodule.

In Fig. 1b shows the nodule resembles a sharp bell shaped. Based on this observation a Gaussian shape was used for the synthetic nodule structure.

This shape has been used as a structural base in other experiments involving synthetic nodules. The magnitude and standard deviation of the Gaussian are all parameters that can be manipulated. The following formulas are used to create the Gaussian that forms the basis for the synthetic nodule.

$$G(x,y) = e^{-(x^2+y^2)/2\sigma^2}$$

This result is then sampled to create an MxN matrix, G[m,n] centred on the origin. The samples are taken using Δx and Δy equal to 1 as the sampling period. The Gaussian that is created is a perfectly symmetric 2D intensity image. The next step in the creation of the synthetic lung nodule addresses this issue. A random,

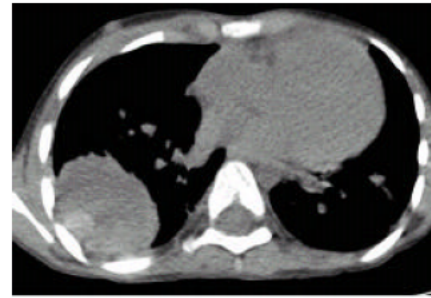


Fig. 1a: CT image with nodules

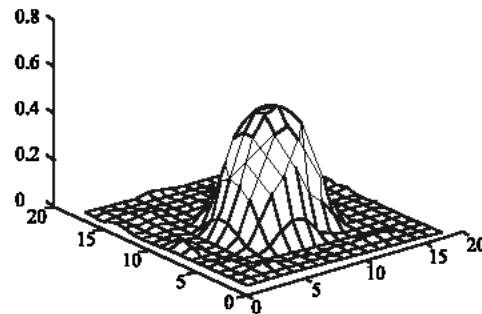


Fig. 1b: 3D mesh for real nodule

asymmetric matrix is added to the Gaussian to provide it with an authentic look (Brown *et al.*, 2001).

$$R[m, n] = \text{random}_{m,n}$$

Random<sub>m,n</sub> [-a,a], distributed uniformly

$$F[m, n] = \alpha \times G[m,n] + \beta \times R[m, n]$$

α and β are scaling terms. The final step is to take the modified Gaussian, F[m, n] and insert it into a real CT image. This is done using a Graphical User Interface (GUI) that reads in the DICOM image data. To blend the nodule smoothly into the image any values of the nodule that are less than those of the image at the insertion coordinates are replaced with the original image value. The parameters that determine the appearance of the nodule are accessible in the GUI (Vernon, 1991). These parameters are the peak intensity and standard deviation of the base Gaussian, the dimensions M and N of the sampling matrix and the interval of the random matrix. The process of inserting the nodule involves adjusting the parameters until the inserted nodule appears as desired by the user (Hom, 1986).

#### RESULTS AND DISCUSSION

A CT image of a patient, who has lung cancer, was collected from a leading medical institute in India for this



Real nodule

Fig. 2: Real nodule present in the CT image

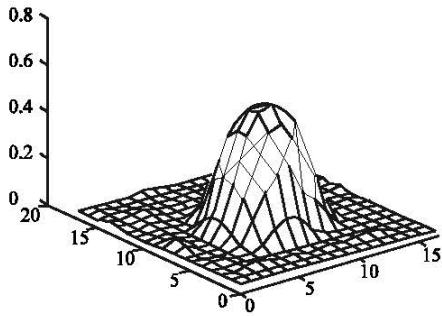


Fig. 3a: 3D mesh for real nodule

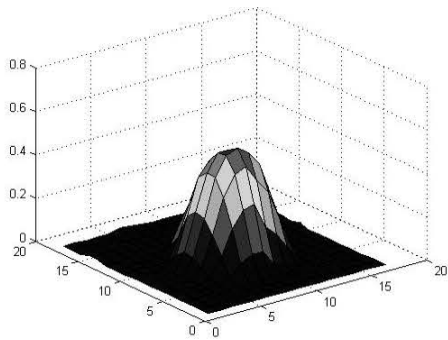


Fig. 3b: 3D surface for realnodule

experiment during the mid of year 2005. Identity is not disclosed honouring the institute sentiments. We developed a software application using MATLAB to analyses the lung nodules. This application has following features:

Identify the real nodules in the CT image. The Fig. 2 shows the real nodule present in the CT image.

The Fig. 3a and b shows a 3D mesh and surface of real lung nodule.

Using Gaussian structure (a) and random asymmetric matrix a synthetic nodule is created.

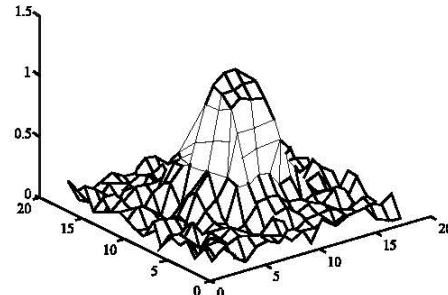


Fig. 4a: 3D mesh for synthetic nodule

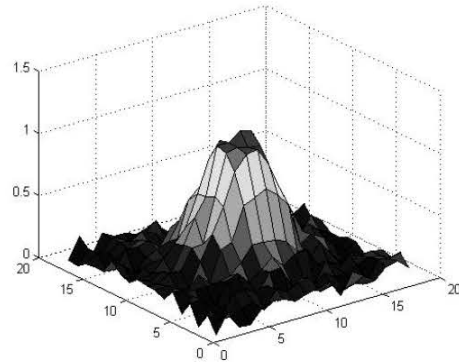


Fig. 4b: 3D surface for synthetic nodule

Real nodule                      Synthetic nodule



Fig. 5: Image containing real and synthetic nodules

A synthetic nodule, which developed using Gaussian, is inserted into CT image (Fig. 4a and b). The Fig. 5 shows an inserted synthetic nodule and real nodule of the CT image.

**CONCLUSIONS**

This software application provides a foundation for the development of a lung nodule segmentation technique

as we have experimented using Gaussian structure, which can help to provide a better technique than, would have been possible with only clinical data. However this study does not experiment with various degrees of CT images. No doubt, there a need for extension of this work with N number of CT images and storing the result into the database will be more useful for lung nodule research community.

## REFERENCES

- Armato, S., M.L. Giger, C.J. Morgan, J.T. Blackbrun, K. Doi, and H. Mac Mahon, 1999. Computerized detection of pulmonary nodules on CT scans. *Imaging and Therapeutic Techol.*, pp: 1303-1311.
- Brown, M. M.F. McNitt-Gray, J.G. Goldin, R.D. Suh, J.W. Sayre and D.R. Aberle, 2001. Patient-specific models for lung nodule detection and surveillance in CT image. *IEEE Transactions on Medical Imaging*, pp: 1242-1250.
- Bullitt, E. and S.R. Aylward, 2001. Analysis of Time-Varying Images Using 3D Vascular Models, *Proceedings of the 30th Applied Imagery Pattern Recognition Workshop*, pp: 0009-0013.
- Caselle, V., F. Catt, T. Coll and F. Dibos, 1993. A geometric model for active contours in image processing. *Numerische Mathematik*, 66: 1-31.
- Dajnowiec, M. and J. Alirezaie, 2004. A computer method for synthesizing lung nodules. *IEEE Canadian Conference on Electrical and Computer Engineering*, pp: 1325-1328.
- Davies, E. 1990. *Machine Vision: Theory, Algorithms and Practicalities*, Academic Press, pp: 42 - 44.
- Gonzalez, R. and R. Woods, 1992. *Digital Image Processing*, Addison-Wesley Publishing Company, pp: 191-198.
- Horn, B., 1986. *Robot Vision*, MIT Press, pp: 20-56.
- Kanazawa, K., Y. Kawata., N. Niki, H. Satoh, H. Ohamatsu and R. Kakinuma, 1998. Computer-aided diagnosis for pulmonary nodules based on helical CT image. *Proceeding of the international Conference on Pattern recognition*, 2;1683-1685.
- Nakamura, Y., G. Fukano, H. Takizawa and S. Mizuno, 2004. Eigen Nodule: View-based Recognition of Lung Nodule in Chest X-ray CT Images Using Subspace Method, *Proceedings of the 17th International Conference on Pattern Recognition*, pp: 681-684.
- Stewart, B. W. and P. Kleihues, 2003. *EDS World Cancer Report*, IARC Press. Lyon , pp: 22-47.
- Takizawa, H. and S. Yamamoto, 2002. Recognition of Lung Nodules from X-ray CT Images Using 3D Markov Random Field Models, *Proceedings of the 16th International Conference on Pattern Recognition*, pp: 10099-10102.
- Vernon, D., 1991. *Machine Vision*, Prentice-Hall, pp: 59-61.
- Zhao, B., G. Gamsu, M.S. Ginsbers, L. Jiang and L.H. Schwartz, 2003. Automatic detection of small lung nodules on CT utilizing a local density maximum algorithm. *J. Applied Clin. Med. Phys.*, 4: 249-260.
- Zrimec, T. and S. Busayarat, 2004. 3-D Modeling and Visualization of Human Lung. *Proceedings of the 2nd International Symposium on 3D Data Processing, Visualization, and Transmission*, pp: 110-115.
- Zwirewich, C. S. Vedal, R. R. Miller and N.L. Muller, 1991. Solitary pulmonary nodule: High-resolution CT and radiological-pathologic correlation. *Radiology*, pp: 469-476.